Published in final edited form as:
Am J Psychiatry. 2012 July 1; 169(7): . doi:10.1176/appi.ajp.2012.11111627.

Cortical thinning in psychopathy

Martina Ly[1,2], **Julian C. Motzkin**[1,2], **Carissa L. Philippi**[1], **Gregory R. Kirk**[1,3], **Joseph P. Newman**[4], **Kent A. Kiehl**[5,6], and **Michael Koenigs**[1,*]

[1]Department of Psychiatry, University of Wisconsin-Madison, 6001 Research Park Blvd., Madison, Wisconsin, 53719, USA

[2]Neuroscience Training Program, University of Wisconsin-Madison, 1300 University Ave., Madison, Wisconsin, 53706, USA

[3]Waisman Center, University of Wisconsin-Madison, 1500 Highland Ave., Madison, Wisconsin, 53705, USA

[4]Department of Psychology, University of Wisconsin-Madison, 1202 West Johnson St., Madison, Wisconsin, 53706, USA

[5]The non-profit MIND Research Network, a subsidiary of Lovelace Biomedical and Environmental Research Institute, 1101 Yale Boulevard NE, Albuquerque, New Mexico, 87131, USA

[6]Departments of Psychology and Neuroscience, University of New Mexico, 1 University of New Mexico MSC03 2220, Albuquerque, New Mexico, 87131, USA

Abstract

Objective—Psychopathy is a personality disorder associated with severely antisocial behavior and a host of cognitive and affective deficits. The neuropathological basis of the disorder has not been clearly established. Cortical thickness is a sensitive measure of brain structure that has been used to identify neurobiological abnormalities in a number of psychiatric disorders. The purpose of this study is to evaluate cortical thickness and corresponding functional connectivity in criminal psychopaths.

Method—Using T1 MRI data, we computed cortical thickness maps in a sample of adult male prison inmates selected based on psychopathy diagnosis (n=21 psychopathic inmates, n=31 non-psychopathic inmates). Using rest-fMRI data from a subset of these inmates (n=20 psychopathic inmates, n=20 non-psychopathic inmates), we then computed functional connectivity within networks exhibiting significant thinning among psychopaths.

Results—Relative to non-psychopaths, psychopaths exhibited significantly thinner cortex in a number of regions, including left insula and dorsal anterior cingulate cortex, bilateral precentral gyrus, bilateral anterior temporal cortex, and right inferior frontal gyrus. These neurostructural differences were not due to differences in age, IQ, or substance abuse. Psychopaths also exhibited a corresponding reduction in functional connectivity between left insula and left dorsal anterior cingulate cortex.

Conclusions—Psychopathy is associated with a distinct pattern of cortical thinning and reduced functional connectivity.

*Corresponding author; mrkoenigs@wisc.edu.

Conflicts of Interest: The authors report no competing interests.

INTRODUCTION

Psychopathy is a mental health disorder characterized by callous and impulsive antisocial behavior. Present in roughly a quarter of adult prison inmates, psychopathy is associated with a disproportionately high incidence of violent crime and recidivism (1). The identification of neural correlates of the disorder could thus have profound implications for the clinical and legal management of psychopathic criminals, as well as for the basic understanding of the biological substrates underlying human social behavior. However, the collection of neuroimaging data from psychopaths involves a number of logistical and methodological challenges—psychopaths are difficult to identify and recruit outside of the criminal justice system, and prison inmates are typically not easily accessible for neuroimaging studies. As a result, such studies have commonly been beset by inadequately small sample sizes, substandard subject assessments and classification, poorly matched comparison subjects, and (predictably) limited convergence of findings (see 2 for review). In this study, we overcome these major limitations through the use of a mobile magnetic resonance imaging (MRI) system within a correctional facility. We collected MRI data from a relatively large sample of well-characterized prison inmates to identify structural and functional differences between psychopathic and non-psychopathic offenders' brains.

Given the complex psychological profile of psychopaths, researchers have proposed dysfunction in a number of cortical and subcortical regions (3, 4). In addition to well-documented deficits in basic emotional responsiveness (5–8), which perhaps suggest dysfunction in subcortical structures like the amygdala (9) and ventral striatum (10), psychopathy is also associated with abnormalities in higher-order cognitive functions, such as attentional control (11, 12), reversal learning (13), and linguistic processing (14, 15). This constellation of deficits suggests dysfunction in frontotemporal cortical areas, particularly orbitofrontal cortex, ventromedial prefrontal cortex, anterior cingulate cortex, insula, and anterior temporal cortex. The aim of the present study is to assess cortical brain structure and corresponding function in psychopathy.

In recent years, the measurement of cortical thickness has been proven as an effective means of identifying neural correlates of psychiatric disorders. For example, distinct regional patterns of cortical thinning have been associated with depression (16), post-traumatic stress disorder (17, 18), autism (19, 20), schizophrenia (21), and subclinical trait anxiety (22, 23). Here, we demonstrate a characteristic pattern of cortical thinning in psychopathy, as well as a corresponding deficit in functional connectivity.

METHOD

Participants

Participants were adult male inmates recruited from a medium-security Wisconsin correctional institution. Inmates were eligible if they met the following criteria: under 45 years of age, IQ greater than 70, no history of psychosis or bipolar disorder, and not currently taking psychotropic medications. Informed consent was obtained both orally and in writing. During the consent procedure, it was emphasized to the inmates that their participation in the research study is voluntary, that they may refuse participation at any time, and that their decision to participate would not be recorded in their prison file, nor would it in any way affect their status within the correctional system. To protect confidentiality, each inmate's data was associated with a unique numerical code, rather than personally identifiable information such as name or prison identification number. Inmates were paid approximately $7 per hour for their participation. Of the 57 inmates who were invited to participate in this MRI study (all previously assessed as psychopathic or non-psychopathic; see below), 52 provided consent and participated.

The Psychopathy Checklist-Revised (PCL-R) (1) was used to assess psychopathy. The PCL-R assessment involves a 60–90 minute interview and file review to obtain information used to rate 20 psychopathy-related items as 0, 1, or 2, depending on the degree to which each trait characterizes the individual. A substantial literature supports the reliability and validity of PCL-R assessments with incarcerated offenders (1). To evaluate interrater reliability, a second rater who was present during interviews provided independent PCL-R ratings for 8 inmates. The intraclass correlation coefficient was 0.85. PCL-R Factor 1 and 2 scores were computed following procedures outlined in the PCL-R manual (1). Participants were assessed for substance use disorder with the Structured Clinical Interview for DSM-IV Disorders (24) (Table 1).

Participant Groups

Participants were recruited for this MRI study based on their PCL-R scores. Psychopathic inmates had PCL-R scores of 30 or greater, while non-psychopathic inmates had PCL-R scores of 20 or less (1). (The use of these cut scores affords clear distinction between high and low levels of psychopathy, but precludes the correlation of imaging data with PCL-R factor or facet scores, which would require a more continuous range of PCL-R scores.) Group characteristics are presented in Table 1.

MRI Data Collection

All MR imaging data were acquired using the Mind Research Network's mobile Siemens 1.5 T Avanto Mobile MRI System with advanced SQ gradients (max slew rate 200T/m/s, 346 T/m/s vector summation, rise time 200 μs) equipped with a 12-element head coil. Head motion was limited using padding and restraint. All prisoners were scanned on correctional facility grounds.

A high-resolution T1-weighted structural image was acquired for each subject using a four-echo magnetization-prepared rapid gradient-echo (MPRAGE) sequence (TR = 2530; TE = 1.64, 3.5, 5.36, 7.22 ms; flip angle = 7°, FOV = 256 × 256 mm, matrix = 128 × 128, slice thickness = 1.33 mm, no gap, voxel size = 1 × 1 × 1.33 mm, 128 interleaved sagittal slices). All four echoes were averaged into a single high-resolution image.

Resting state functional images were collected while subjects lay still and awake, passively viewing a fixation cross. T2*-weighted gradient-echo echoplanar functional images (EPIs) were acquired with the following parameters: TR = 2000 ms, TE = 39 ms, flip angle = 75 °, FOV = 24 × 24 cm, matrix = 64 × 64, slice thickness = 4 mm, gap = 1 mm, voxel size = 3.75 mm × 3.75 mm × 5 mm, 27 sequential axial oblique slices. Resting-state scans lasted 5.5 minutes (158 volumes). Rest fMRI data were available for a subset of n=20 psychopathic inmates and n=20 non-psychopathic inmates.

Measurement of Cortical Thickness

The averaged T1-weighted images were processed using FreeSurfer v5.0 (Athinoula A. Martinos Center for Biomedical Imaging and CorTechs Labs©, http://www.nmr.mgh.harvard.edu/freesurfer), as previously described (25–31). Briefly, the automated procedure includes skull-stripping, registration, intensity normalization, Talairach transformation, tissue segmentation, and surface tessellation. The pial surface of each hemisphere was computed by deforming the tessellated white matter surface outward toward the gray matter/cerebrospinal fluid boundary. The distance between the white matter surface and pial surface yields an estimate of cortical thickness at each vertex. This method of obtaining thickness of the cortex has been validated histologically (32) and by manual measurement on MRI sections (33, 34).

The reconstructed cortical surfaces for each study participant were then aligned to produce an average cortical surface. A mapping was thus obtained between each vertex on the average surface and the corresponding vertex on the surface of each subject's cortical reconstruction. The cortical thickness maps for each subject were then resampled onto the average surface and smoothed with a 10 mm full-width/half-maximum Gaussian kernel.

Statistical Analysis of Cortical Thickness

For each group (psychopaths and non-psychopaths), we computed a linear model of cortical thickness as a function of age at every vertex on the surface. Parametric maps derived from this between-group comparison in cortical thickness, while regressing out the effect of age, were overlain on the average cortical surface. Next, an automatic clustering algorithm was applied to segregate all points on the average cortical surface with an uncorrected p-value < 0.01 (Figure 1) into clusters and then to compute a clusterwise p-value correction by means of a Monte Carlo simulation to determine clusters with a corrected clusterwise significance of $p < 0.05$ (Figure 2) (35, 36).

fMRI Data Processing

Preprocessing—All fMRI data analysis was performed using AFNI (37) and FSL (http://www.fmrib.ox.ac.uk/fsl/). EPI volumes were slice time corrected using the first slice as a reference (sequential acquisition, fourier interpolation) and motion corrected by rigid body alignment to the first EPI acquisition. Any subject with motion greater than 4 mm in any direction was excluded from further analysis. The first 3 volumes were omitted from the EPI time series and the data were despiked to remove extreme time series outliers. Time series data were bandpass filtered ($0.009 < f < 0.08$) before spatially smoothing with a 4-mm full width at half maximum (FWHM) Gaussian kernel. EPI time series data and high-resolution T1 images were normalized to the Talairach coordinate system (38) using a 12-parameter linear warp and the EPI data were resampled to 3 mm cubic voxels for subsequent functional connectivity analyses. Normalized T1 anatomical images were segmented into gray matter, white matter, and cerebrospinal fluid (CSF) segments using FAST in FSL (39). White matter and CSF segments were used as masks to extract a representative time series from each tissue type.

ROI Selection and Correlation analysis—The cortical thickness analysis revealed a total of 13 areas of significantly reduced thinning among psychopaths (see Results for full description). Among these 13 areas, three pairs of areas normally exhibit significant functional connectivity (within the pair): (1) right and left precentral gyri (40), (2) right and left temporal poles (41), and (3) left insula and left dorsal anterior cingulate cortex (42, 43). To calculate functional connectivity within each of these pairs, we first constructed seed ROIs at the site of maximum p-value significance of cortical thinning in each area. We next constructed anatomical masks for the corresponding region within the pair (e.g., the seed in right precentral gyrus was paired with a mask in left precentral gyrus, and vice versa). The masks were created using the Harvard-Oxford anatomical atlas included in FSL (44). For the left dorsal anterior cingulate mask, the original anterior cingulate mask from the Harvard-Oxford atlas was edited in FSL to exclude the subgenual anterior cingulate. Functional connectivity was assessed by computing correlations within each mask for the mean time series derived separately from the corresponding seed ROI. The mean time series was included in a GLM with eight regressors of no interest, including six motion parameters (3 translations, 3 rotations) obtained from the rigid body alignment of EPI volumes, the ventricular time series acquired by averaging across the CSF mask, the white matter time series acquired by averaging across the white matter mask, and a second order polynomial to model baseline signal and slow drift. Voxelwise correlation coefficients for each ROI were

converted to z scores via Fisher's r to z transform and the resulting z-score maps were entered into second level statistical analyses.

Statistical Analyses of Correlation maps—To compare functional connectivity between psychopathic and non-psychopathic inmates, we performed unpaired two-sample t-tests on the z-score maps derived from each seed/mask pair. Group difference maps were corrected for multiple comparisons using cluster-extent thresholding at an uncorrected $p<0.005$, $\alpha=0.05$. Cluster extents were computed using Monte Carlo simulations implemented in the 3dClustSim program (AFNI). Group correlation maps were overlaid on the normalized mean anatomical image. All coordinates are reported in Talairach space.

RESULTS

Psychopaths had significantly thinner cortex than non-psychopaths in a number of areas (Figure 1, Figure 2, Table 2).

The largest and most significant clusters were in left insula, left dorsal anterior cingulate cortex, bilateral precentral gyrus, bilateral temporal pole, and right inferior frontal gyrus. There were no areas where non-psychopaths had significantly thinner cortex than psychopaths.

Given that psychopaths had a somewhat higher rate of substance use disorder than non-psychopaths in our sample (Table 1), we performed a follow-up analysis to determine whether any of the observed differences in cortical thickness between psychopaths and non-psychopaths could be due to differences in rates of substance use disorder. To address this question, we grouped inmates based on substance use disorder diagnosis: inmates with substance use disorder diagnosis (n=26) versus inmates with no substance use disorder diagnosis (n=26). Using the same statistical criteria as the psychopath versus non-psychopath group analysis, we found no areas of significantly different cortical thickness between the two groups of inmates (i.e., no areas survived the clusterwise threshold of $p < 0.05$). Therefore, we conclude that the observed results are in fact due to different levels of psychopathy, rather than different rates of substance use disorder.

To determine whether the observed differences in cortical thickness were associated with corresponding reductions in functional connectivity, we assessed functional connectivity between three pairs of regions: (1) right and left precentral gyri, (2) right and left temporal pole, and (3) left insula and left dorsal anterior cingulate cortex. Each of these pairs of regions exhibited significantly thinner cortex in psychopaths, and each of these pairs is known to exhibit significant functional connectivity in normal subjects (40–43). Among these pairs of regions, only the left insula and left dorsal anterior cingulate cortex had significantly reduced functional connectivity in psychopaths relative to non-psychopaths (Figure 3).

DISCUSSION

This study is the first to examine thickness throughout the entire cortex in a sizeable sample of stringently classified psychopaths (n=21 with PCL-R≥30). Relative to non-psychopathic prison inmates, psychopaths exhibited discrete areas of significant cortical thinning. The area of greatest difference in cortical thickness was the left insula. This finding aligns closely with a recent study showing that violent offenders exhibit gray matter volume reductions specifically in left anterior insula (relative to non-offenders matched for substance use disorder), and that psychopathy severity is negatively correlated with left insula volume (45). In addition, a previous study of gray matter structure in psychopathy

identified reductions in insula, among other brain regions (46). These convergent results implicate thinning in insula as a robust neural correlate of psychopathic behavior.

Interestingly, insula is strongly interconnected with a second set of areas in which we also found significant cortical thinning among psychopaths: the dorsal anterior cingulate cortex and adjacent medial superior frontal gyrus. Studies of functional connectivity have identified a circuit comprised principally by nodes in anterior insula/frontal operculum and dorsal anterior cingulate cortex/medial superior frontal gyrus (42, 43). Furthermore, dorsal anterior cingulate cortex/medial superior frontal gyrus and anterior insula/frontal operculum are the two areas of the brain with the highest numbers of Von Economo neurons, a cell-type that is specifically found in great apes and especially humans (47, 48). Based on the functional and cytological links between these two areas, we see the corresponding cortical thinning in these two areas as potential evidence for a comprised insula-dorsal anterior cingulate circuit in psychopathy. In strong support of this argument, we found significantly lower functional connectivity between left insula and left dorsal anterior cingulate among psychopaths. Although the function of this insula-dorsal anterior cingulate circuit remains to be fully elucidated, human fMRI studies suggest a role in the flexible control of goal-directed behavior via signaling for top-down control (43, 49, 50). It is noteworthy that behavioral and psychophysiological studies of psychopaths have previously demonstrated abnormalities in the flexibility of goal-directed attention (e.g., 11, 12, 51). Dysfunction in the insula-dorsal anterior cingulate circuit could conceivably be a neural correlate of this behavioral characteristic. Further work, particularly with measures of task-related functional connectivity in psychopaths, will be necessary to more directly investigate this hypothesis.

We also observed a robust difference in cortical thickness between psychopaths and non-psychopaths in precentral gyrus bilaterally. Although precentral gyrus is primarily known as an area for motor planning and execution—and thus not typically theorized to play any meaningful role in psychopathy—there is mounting evidence that precentral gyrus may indeed mediate functions germane to psychopathy. Recent studies have associated precentral gyrus activity with impulsivity in juvenile offenders (52), abstract emotional meaning (53), empathy for pain (54), and value signals during decision-making (55). Moreover, thinning in precentral gyrus has been identified in studies of individuals with psychopathic characteristics (56, 57). One previous study associated violence and antisocial personality disorder with thinning specifically in precentral gyrus (56), while a second study found thinner precentral gyrus in a community sample with relatively high psychopathy scores (57). Using a stringent and well-validated subject classification scheme, here we demonstrate bilateral precentral thinning in psychopathic criminals.

Another set of areas where we found significant thinning bilaterally was the temporal pole and superior temporal gyrus. This finding converges with functional imaging data showing reduced activity in anterior, superior temporal lobe in psychopaths during lexical decision-making (15) and moral judgment (58), as well as with a recent voxel-based morphometry (VBM) study showing a negative correlation between temporal pole gray matter volume and psychopathy severity in a large sample of prison inmates (59). In addition, one previous study found reduced thickness in bilateral temporal poles in a community sample with relatively high psychopathy scores (57), while an earlier VBM study found relatively specific volume reductions in bilateral temporal pole among incarcerated psychopaths relative to non-psychopaths (60). However, the non-psychopathic comparison group in this previous VBM study was not matched for incarceration status, IQ, or substance use history. The present results and those of Ermer et al. (59), which fully account for these important variables, more definitively establish a link between psychopathy and thinning in temporal pole.

Cortical thinning was also observed in the right inferior frontal gyrus of psychopaths, consistent with a previous study (57). Growing evidence suggests a role for inferior frontal gyrus in social cognition. Since the discovery of mirror neurons in the monkey area F5 (the homologue to human IFG) (61, 62), inferior frontal gyrus has been proposed as potential neural substrate underlying empathy (63). Indeed, autism, a neurodevelopmental disorder featuring deficient empathy and impoverished interpersonal affection, is associated with a lack of "mirror" activity in inferior frontal gyrus (64) as well as reduced inferior frontal gyrus thickness (65) and volume (66). Perhaps the hallmark psychopathic traits of inability to experience empathy and reduced affect are related to thinning in right inferior frontal gyrus.

Finally, we consider how our results relate to two leading neurobiological models of psychopathy. One prominent model proposes primary dysfunction in a circuit comprised of amygdala and ventromedial prefrontal cortex (3, 67). Although our cortical thickness analysis did not include subcortical structures such as amygdala, we did find thinning in anterior and superior temporal cortices, which overlie and densely interconnect with amygdala (68, 69). With respect to ventromedial prefrontal cortex, we found limited evidence of cortical thinning among psychopaths—a small area in the right gyrus rectus that was significant at $p < 0.01$ (uncorrected) but did not survive clusterwise $p < 0.05$ correction. Reduced thickness in ventromedial prefrontal cortex may have been predicted on the basis of recent results from an overlapping inmate sample demonstrating significantly reduced functional connectivity in ventromedial prefrontal cortex among psychopaths (70). In addition, two previous structural imaging studies have associated psychopathy with reduced gray matter in areas adjacent to ventromedial prefrontal cortex, including frontopolar cortex and orbitofrontal cortex (46, 57). The absence of any extensive ventromedial prefrontal cortex thickness difference in the present study suggests that psychopathy may not reliably be associated with a substantial lack of ventromedial prefrontal cortex tissue integrity, but rather, that ventromedial prefrontal cortex may be abnormally connected within the psychopathic brain.

A second prominent neuroanatomical model of psychopathy proposes dysfunction in a broader "paralimbic" network (4). Our data offer mixed support for this model; several areas of significant thinning were located within the paralimbic network (e.g., insula, dorsal anterior cingulate cortex, temporal pole), while several areas were not (e.g., precentral gyrus, lateral occipital cortex, superior frontal gyrus). Future research with multimodal imaging approaches will be necessary to more fully evaluate the extent to which either of these models accurately characterizes the neuropathological basis of the disorder.

In conclusion, this study identifies a constellation of cortical regions that exhibit reduced thickness in psychopathic criminals. These findings are a significant advance toward establishing the neural correlates of psychopathy.

Acknowledgments

This work was supported by a UW-Madison/UW-Milwaukee Intercampus Research Incentive Grant and grants from the National Institutes of Health (MH070539, DA026505, MH086787, MH078980). We thank Keith Harenski for his assistance with MRI data collection. We thank many at the Wisconsin Department of Corrections for making this research possible. We are especially indebted to Deputy Warden Tom Nickel and Dr. Kevin Kallas.

REFERENCES

1. Hare, RD. The Hare psychopathy checklist-revised. 2nd ed. Toronto: Multi-Health Systems; 2003.
2. Koenigs M, Baskin-Sommers A, Zeier J, Newman JP. Investigating the neural correlates of psychopathy: a critical review. Mol Psychiatry. 2011; 16(8):792–799. [PubMed: 21135855]

3. Blair RJ. The amygdala and ventromedial prefrontal cortex: functional contributions and dysfunction in psychopathy. Philos Trans R Soc Lond B Biol Sci. 2008; 363(1503):2557–2565. [PubMed: 18434283]
4. Kiehl KA. A cognitive neuroscience perspective on psychopathy: evidence for paralimbic system dysfunction. Psychiatry Res. 2006; 142(2–3):107–128. [PubMed: 16712954]
5. Lykken DT. A study of anxiety in the sociopathic personality. J Abnorm Psychol. 1957; 55(1):6–10. [PubMed: 13462652]
6. Hare RD. Psychopathy and electrodermal responses to nonsignal stimulation. Biol Psychol. 1978; 6(4):237–246. [PubMed: 708810]
7. Schmauk FJ. Punishment, arousal, and avoidance learning in sociopaths. J Abnorm Psychol. 1970; 76(3):325–335. [PubMed: 4395258]
8. Patrick CJ, Cuthbert BN, Lang PJ. Emotion in the criminal psychopath: fear image processing. J Abnorm Psychol. 1994; 103(3):523–534. [PubMed: 7930052]
9. Birbaumer N, Veit R, Lotze M, Erb M, Hermann C, Grodd W, Flor H. Deficient fear conditioning in psychopathy: a functional magnetic resonance imaging study. Arch Gen Psychiatry. 2005; 62(7): 799–805. [PubMed: 15997022]
10. Buckholtz JW, Treadway MT, Cowan RL, Woodward ND, Benning SD, Li R, Ansari MS, Baldwin RM, Schartzman AN, Shelby ES, Smith CE, Cole D, Kessler RM, Zald DH. Mesolimbic dopamine reward system hypersensitivity in individuals with psychopathic traits. Nat Neurosci. 2010; 13(4):419–421. [PubMed: 20228805]
11. Hiatt KD, Schmitt WA, Newman JP. Stroop tasks reveal abnormal selective attention among psychopathic offenders. Neuropsychology. 2004; 18(1):50–59. [PubMed: 14744187]
12. Zeier JD, Maxwell JS, Newman JP. Attention moderates the processing of inhibitory information in primary psychopathy. J Abnorm Psychol. 2009; 118(3):554–563. [PubMed: 19685952]
13. Budhani S, Richell RA, Blair RJ. Impaired reversal but intact acquisition: probabilistic response reversal deficits in adult individuals with psychopathy. J Abnorm Psychol. 2006; 115(3):552–558. [PubMed: 16866595]
14. Kiehl KA, Hare RD, McDonald JJ, Brink J. Semantic and affective processing in psychopaths: an event-related potential (ERP) study. Psychophysiology. 1999; 36(6):765–774. [PubMed: 10554590]
15. Kiehl KA, Smith AM, Mendrek A, Forster BB, Hare RD, Liddle PF. Temporal lobe abnormalities in semantic processing by criminal psychopaths as revealed by functional magnetic resonance imaging. Psychiatry Res. 2004; 130(1):27–42. [PubMed: 14972366]
16. Peterson BS, Warner V, Bansal R, Zhu H, Hao X, Liu J, Durkin K, Adams PB, Wickramaratne P, Weissman MM. Cortical thinning in persons at increased familial risk for major depression. Proc Natl Acad Sci U S A. 2009; 106(15):6273–6278. [PubMed: 19329490]
17. Geuze E, Westenberg HG, Heinecke A, de Kloet CS, Goebel R, Vermetten E. Thinner prefrontal cortex in veterans with posttraumatic stress disorder. Neuroimage. 2008; 41(3):675–681. [PubMed: 18445532]
18. Woodward SH, Schaer M, Kaloupek DG, Cediel L, Eliez S. Smaller global and regional cortical volume in combat-related posttraumatic stress disorder. Arch Gen Psychiatry. 2009; 66(12):1373–1382. [PubMed: 19996042]
19. Hardan AY, Libove RA, Keshavan MS, Melhem NM, Minshew NJ. A preliminary longitudinal magnetic resonance imaging study of brain volume and cortical thickness in autism. Biol Psychiatry. 2009; 66(4):320–326. [PubMed: 19520362]
20. Schumann CM, Bloss CS, Barnes CC, Wideman GM, Carper RA, Akshoomoff N, Pierce K, Hagler D, Schork N, Lord C, Courchesne E. Longitudinal magnetic resonance imaging study of cortical development through early childhood in autism. J Neurosci. 2010; 30(12):4419–4427. [PubMed: 20335478]
21. van Haren NE, Schnack HG, Cahn W, van den Heuvel MP, Lepage C, Collins L, Evans AC, Huslhoff Pol HE, Kahn RS. Changes in cortical thickness during the course of illness in schizophrenia. Arch Gen Psychiatry. 2011; 68(9):871–880. [PubMed: 21893656]

22. Kuhn S, Schubert F, Gallinat J. Structural correlates of trait anxiety: Reduced thickness in medial orbitofrontal cortex accompanied by volume increase in nucleus accumbens. J Affect Disord. 2011; 134(1–3):315–319. [PubMed: 21705088]
23. Blackmon K, Barr WB, Carlson C, Devinsky O, Dubois J, Pogash D, Quinn BT, Kuzniecky R, Halgren E, Thesen T. Structural evidence for involvement of a left amygdala-orbitofrontal network in subclinical anxiety. Psychiatry Res. 2011
24. First, MB.; Spitzer, RL.; Gibbon, M.; Williams, JBW. Structured Clinical Interview for DSM-IV-TR Axis I Disorders, Research Version, Non-patient Edition. (SCID-I/NP). New York: Biometrics Research, New York State Psychiatric Institute; 2002.
25. Segonne F, Dale AM, Busa E, Glessner M, Salat D, Hahn HK, Fischl B. A hybrid approach to the skull stripping problem in MRI. Neuroimage. 2004; 22(3):1060–1075. [PubMed: 15219578]
26. Fischl B, van der Kouwe A, Destrieux C, Halgren E, Segonne F, Salat DH, Busa E, Seidman LJ, Goldstein J, Kennedy D, Caviness V, Makris N, Rosen B, Dale AM. Automatically parcellating the human cerebral cortex. Cereb Cortex. 2004; 14(1):11–22. [PubMed: 14654453]
27. Fischl B, Liu A, Dale AM. Automated manifold surgery: constructing geometrically accurate and topologically correct models of the human cerebral cortex. IEEE Trans Med Imaging. 2001; 20(1): 70–80. [PubMed: 11293693]
28. Dale AM, Fischl B, Sereno MI. Cortical surface-based analysis. I. Segmentation and surface reconstruction. Neuroimage. 1999; 9(2):179–194. [PubMed: 9931268]
29. Fischl B, Dale AM. Measuring the thickness of the human cerebral cortex from magnetic resonance images. Proc Natl Acad Sci U S A. 2000; 97(20):11050–11055. [PubMed: 10984517]
30. Fischl B, Sereno MI, Dale AM. Cortical surface-based analysis. II: Inflation, flattening, and a surface-based coordinate system. Neuroimage. 1999; 9(2):195–207. [PubMed: 9931269]
31. Fischl B, Sereno MI, Tootell RB, Dale AM. High-resolution intersubject averaging and a coordinate system for the cortical surface. Hum Brain Mapp. 1999; 8(4):272–284. [PubMed: 10619420]
32. Rosas HD, Liu AK, Hersch S, Glessner M, Ferrante RJ, Salat DH, van der Kouwe A, Jenkins BG, Dale AM, Fischl B. Regional and progressive thinning of the cortical ribbon in Huntington's disease. Neurology. 2002; 58(5):695–701. [PubMed: 11889230]
33. Kuperberg GR, Broome MR, McGuire PK, David AS, Eddy M, Ozawa F, Goff D, West WC, Williams SC, van der Kouwe AJ, Salat DH, Dale AM, Fischl B. Regionally localized thinning of the cerebral cortex in schizophrenia. Arch Gen Psychiatry. 2003; 60(9):878–888. [PubMed: 12963669]
34. Salat DH, Buckner RL, Snyder AZ, Greve DN, Desikan RS, Busa E, Morris JC, Dale AM, Fischl B. Thinning of the cerebral cortex in aging. Cereb Cortex. 2004; 14(7):721–730. [PubMed: 15054051]
35. Nichols TE, Holmes AP. Nonparametric permutation tests for functional neuroimaging: a primer with examples. Hum Brain Mapp. 2002; 15(1):1–25. [PubMed: 11747097]
36. Walhovd KB, Moe V, Slinning K, Due-Tonnessen P, Bjornerud A, Dale AM, van der Kouwe A, Quinn BT, Kosofsky B, Greve D, Fischl B. Volumetric cerebral characteristics of children exposed to opiates and other substances in utero. Neuroimage. 2007; 36(4):1331–1344. [PubMed: 17513131]
37. Cox RW. AFNI: software for analysis and visualization of functional magnetic resonance neuroimages. Comput Biomed Res. 1996; 29(3):162–173. [PubMed: 8812068]
38. Talairach, J.; Tournoux, P. Co-planar Stereotaxic Atlas of the Human Brain. New York: Theime Medical; 1988.
39. Zhang Y, Brady M, Smith S. Segmentation of brain MR images through a hidden Markov random field model and the expectation-maximization algorithm. IEEE Trans Med Imaging. 2001; 20(1): 45–57. [PubMed: 11293691]
40. Biswal B, Yetkin FZ, Haughton VM, Hyde JS. Functional connectivity in the motor cortex of resting human brain using echo-planar MRI. Magn Reson Med. 1995; 34(4):537–541. [PubMed: 8524021]

41. Roy AK, Shehzad Z, Margulies DS, Kelly AM, Uddin LQ, Gotimer K, Biswal BB, Castellanos FX, Milham MP. Functional connectivity of the human amygdala using resting state fMRI. Neuroimage. 2009; 45(2):614–626. [PubMed: 19110061]

42. Dosenbach NU, Fair DA, Miezin FM, Cohen AL, Wenger KK, Dosenbach RA, Fox MD, Snyder AZ, Vincent JL, Raichle ME, Schlagger BL, Petersen SE. Distinct brain networks for adaptive and stable task control in humans. Proc Natl Acad Sci U S A. 2007; 104(26):11073–11078. [PubMed: 17576922]

43. Seeley WW, Menon V, Schatzberg AF, Keller J, Glover GH, Kenna H, Reiss AL, Greicius MD. Dissociable intrinsic connectivity networks for salience processing and executive control. J Neurosci. 2007; 27(9):2349–2356. [PubMed: 17329432]

44. Smith SM, Jenkinson M, Woolrich MW, Beckmann CF, Behrens TE, Johansen-Berg H, Bannister PR, Matthews PM. Advances in functional and structural MR image analysis and implementation as FSL. Neuroimage. 2004; 23(Suppl 1):S208–S219. [PubMed: 15501092]

45. Schiffer B, Muller BW, Scherbaum N, Hodgins S, Forsting M, Wiltfang J, Gizewski ER, Leygraf N. Disentangling structural brain alterations associated with violent behavior from those associated with substance use disorders. Arch Gen Psychiatry. 2011; 68(10):1039–1049. [PubMed: 21646569]

46. de Oliveira-Souza R, Hare RD, Bramati IE, Garrido GJ, Azevedo Ignacio F, Tovar-Moll F, Moll J. Psychopathy as a disorder of the moral brain: fronto-temporo-limbic grey matter reductions demonstrated by voxel-based morphometry. Neuroimage. 2008; 40(3):1202–1213. [PubMed: 18289882]

47. Nimchinsky EA, Gilissen E, Allman JM, Perl DP, Erwin JM, Hof PR. A neuronal morphologic type unique to humans and great apes. Proc Natl Acad Sci U S A. 1999; 96(9):5268–5273. [PubMed: 10220455]

48. von Economo C. A new type of special cells of the cingulate and insular lobes. Z Ges Neurol Psychiatr. 1926; 100:707–712.

49. Menon V, Uddin LQ. Saliency, switching, attention and control: a network model of insula function. Brain structure & function. 2010; 214(5–6):655–667. [PubMed: 20512370]

50. Wilk HA, Ezekiel F, Morton JB. Brain regions associated with moment-to-moment adjustments in control and stable task-set maintenance. Neuroimage. 2011

51. Newman JP, Curtin JJ, Bertsch JD, Baskin-Sommers AR. Attention moderates the fearlessness of psychopathic offenders. Biol Psychiatry. 2010; 67(1):66–70. [PubMed: 19793581]

52. Shannon BJ, Raichle ME, Snyder AZ, Fair DA, Mills KL, Zhang D, Bache K, Calhoun VD, Nigg JT, Nagel BJ, Stevens AA, Kiehl KA. Premotor functional connectivity predicts impulsivity in juvenile offenders. Proc Natl Acad Sci U S A. 2011; 108(27):11241–11245. [PubMed: 21709236]

53. Moseley R, Carota F, Hauk O, Mohr B, Pulvermuller F. A Role for the Motor System in Binding Abstract Emotional Meaning. Cereb Cortex. 2011

54. Fecteau S, Pascual-Leone A, Theoret H. Psychopathy and the mirror neuron system: preliminary findings from a non-psychiatric sample. Psychiatry Res. 2008; 160(2):137–144. [PubMed: 18599127]

55. Sul JH, Jo S, Lee D, Jung MW. Role of rodent secondary motor cortex in value-based action selection. Nat Neurosci. 2011; 14(9):1202–1208. [PubMed: 21841777]

56. Narayan VM, Narr KL, Kumari V, Woods RP, Thompson PM, Toga AW, Sharma T. Regional cortical thinning in subjects with violent antisocial personality disorder or schizophrenia. Am J Psychiatry. 2007; 164(9):1418–1427. [PubMed: 17728428]

57. Yang Y, Raine A, Colletti P, Toga AW, Narr KL. Abnormal temporal and prefrontal cortical gray matter thinning in psychopaths. Mol Psychiatry. 2009; 14(6):561–562. 55. [PubMed: 19455172]

58. Harenski CL, Harenski KA, Shane MS, Kiehl KA. Aberrant neural processing of moral violations in criminal psychopaths. J Abnorm Psychol. 2010; 119(4):863–874. [PubMed: 21090881]

59. Ermer E, Cope LM, Nyalakanti PK, Calhoun VD, Kiehl KA. Aberrant paralimbic gray matter in criminal psychopathy. Journal of Abnormal Psychology. in press.

60. Muller JL, Ganssbauer S, Sommer M, Dohnel K, Weber T, Schmidt-Wilcke T, Hajak G. Gray matter changes in right superior temporal gyrus in criminal psychopaths. Evidence from voxel-based morphometry. Psychiatry Res. 2008; 163(3):213–222. [PubMed: 18662867]

61. Gallese V, Fadiga L, Fogassi L, Rizzolatti G. Action recognition in the premotor cortex. Brain. 1996; 119(Pt 2):593–609. [PubMed: 8800951]
62. Rizzolatti G, Fadiga L, Gallese V, Fogassi L. Premotor cortex and the recognition of motor actions. Brain research Cognitive brain research. 1996; 3(2):131–141. [PubMed: 8713554]
63. Iacoboni M. Imitation, empathy, and mirror neurons. Annual review of psychology. 2009; 60:653–670.
64. Dapretto M, Davies MS, Pfeifer JH, Scott AA, Sigman M, Bookheimer SY, Iacoboni M. Understanding emotions in others: mirror neuron dysfunction in children with autism spectrum disorders. Nat Neurosci. 2006; 9(1):28–30. [PubMed: 16327784]
65. Hadjikhani N, Joseph RM, Snyder J, Tager-Flusberg H. Anatomical differences in the mirror neuron system and social cognition network in autism. Cereb Cortex. 2006; 16(9):1276–1282. [PubMed: 16306324]
66. Yamasaki S, Yamasue H, Abe O, Suga M, Yamada H, Inoue H, Kasai K. Reduced gray matter volume of pars opercularis is associated with impaired social communication in high-functioning autism spectrum disorders. Biol Psychiatry. 2010; 68(12):1141–1147. [PubMed: 20801427]
67. Blair RJ. The amygdala and ventromedial prefrontal cortex in morality and psychopathy. Trends Cogn Sci. 2007; 11(9):387–392. [PubMed: 17707682]
68. Amaral DG, Price JL. Amygdalo-cortical projections in the monkey (Macaca fascicularis). J Comp Neurol. 1984; 230(4):465–496. [PubMed: 6520247]
69. Herzog AG, Van Hoesen GW. Temporal neocortical afferent connections to the amygdala in the rhesus monkey. Brain Res. 1976; 115(1):57–69. [PubMed: 824015]
70. Motzkin JC, Newman JP, Kiehl KA, Koenigs M. Reduced prefrontal connectivity in psychopathy. J Neurosci. 2011; 31(48):17348–17357. [PubMed: 22131397]
71. Chapman LJ, Chapman JP. The measurement of handedness. Brain and cognition. 1987; 6(2):175–183. [PubMed: 3593557]
72. Zachary, RA. Shipley Institute of Living Scale: Revised Manual. Los Angeles: Western Psychological Services; 1986.

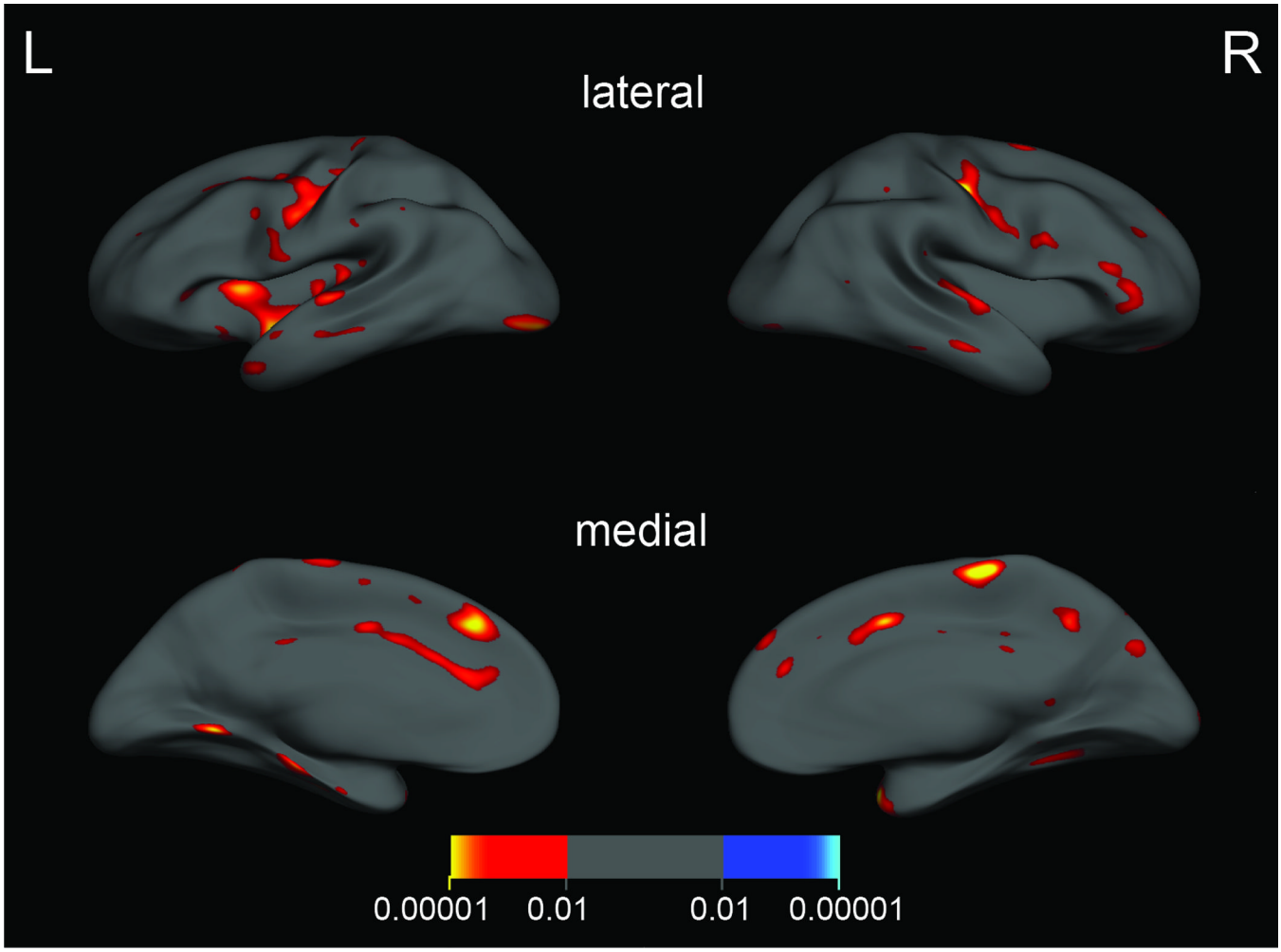

Figure 1.
Areas of significantly thinner cortex in psychopaths ($p < 0.01$, uncorrected). The color bar indicates p-value.

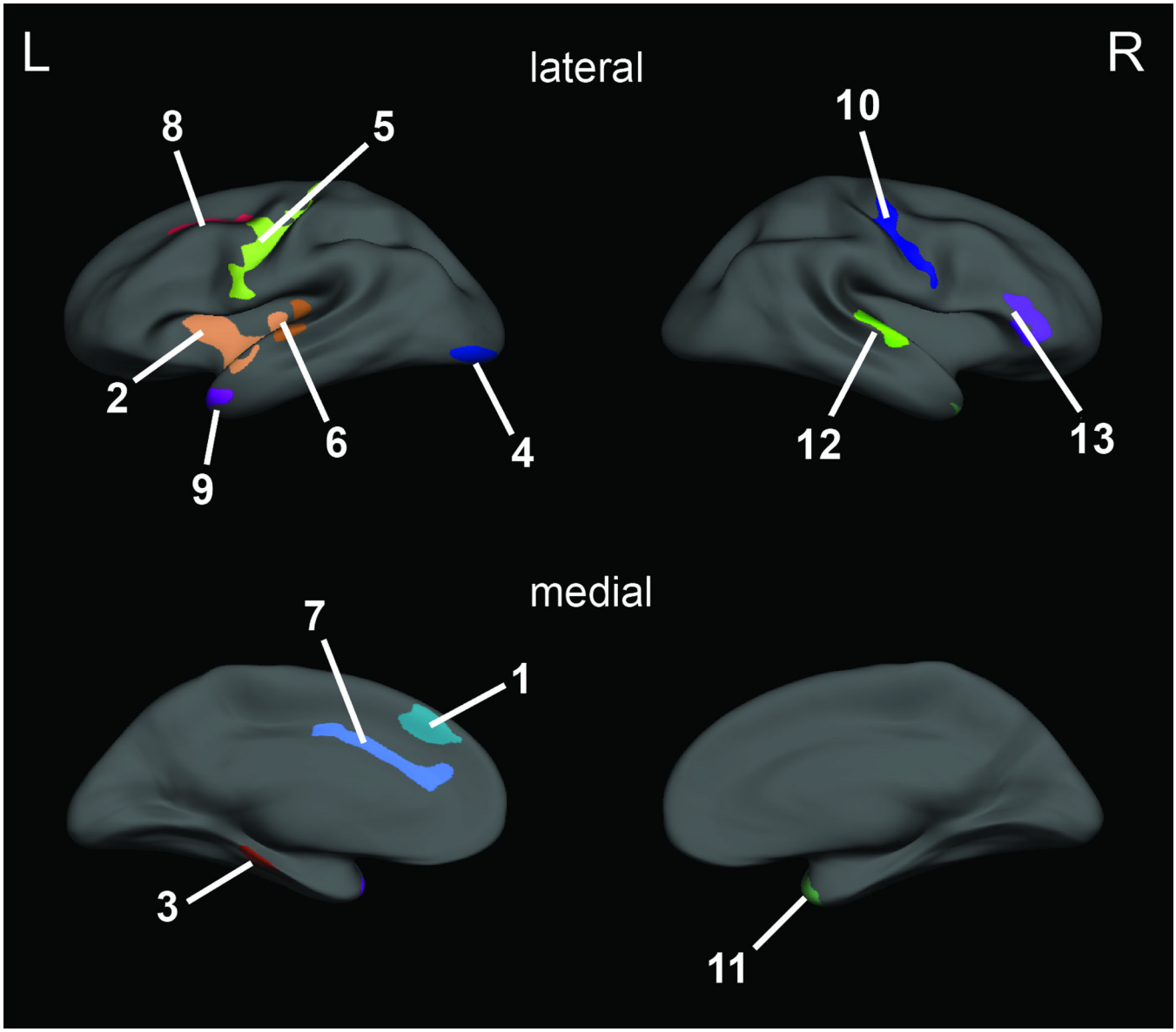

Figure 2.
Clusters of significantly thinner cortex in psychopaths ($p < 0.05$, corrected). Each color represents a distinct cluster. Numbers refer to cluster characteristics in Table 2.

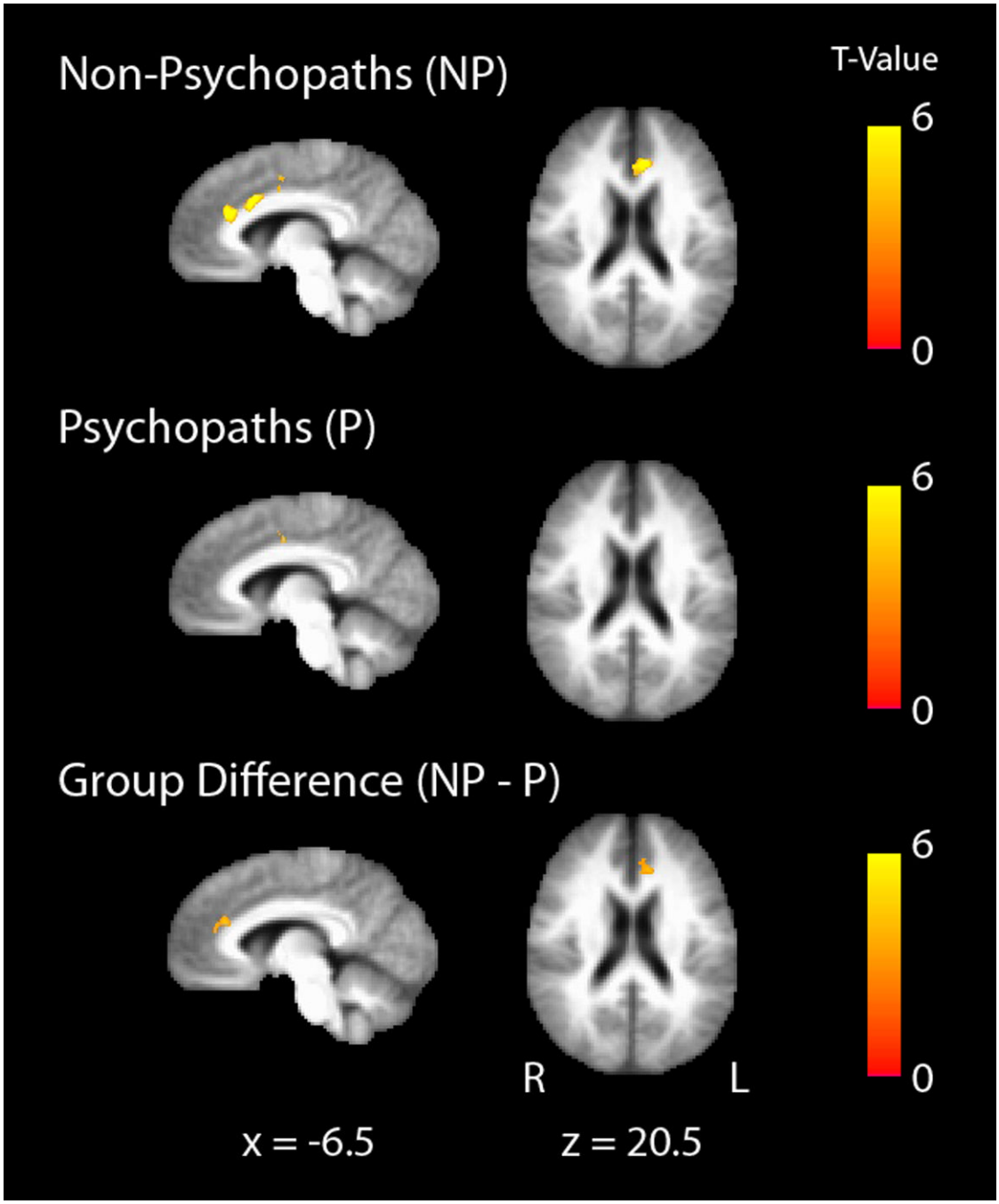

Figure 3.
Functional connectivity between the left anterior insula and left dorsal anterior cingulate cortex is reduced in psychopaths. Mean left insula-dorsal anterior cingulate connectivity maps for non-psychopaths (top row) and psychopaths (middle row) are shown separately on the group mean anatomical image, thresholded at a cluster corrected $p<0.05$. Scale bars depict the uncorrected T-statistic. The group difference map (bottom row) indicates an area in dorsal anterior cingulate where non-psychopaths have significantly greater connectivity with anterior insula than psychopaths ($x = -12$, $y = 30$, $z = 20.5$, cluster size = 41 voxels).

Table 1

Participant group characteristics

Variable	Non-psychopaths (n=31)		Psychopaths (n=21)		p
	Mean	**S.D.**	**Mean**	**S.D.**	
Demographic					
Age	32.1	7.7	32.7	6.7	0.77
Race (% Cauc)	93.5%		76.2%		0.19
Handed[a] (% Right)	93.5%		95.2%		0.99
Neuropsychological					
IQ[b]	101.7	12.3	100.1	10.3	0.64
Digit Span Backward	6.9	2.0	6.8	3.3	0.90
Anxiety/Neg Affect[c]	11.0	9.3	14.0	8.6	0.25
Psychopathy					
PCL-R total	13.5	4.0	31.8	1.7	<0.001
Factor 1	4.6	2.2	11.8	1.7	<0.001
Factor 2	7.1	3.2	17.2	1.4	<0.001
Substance Abuse[d]					
Alcohol					
Prevalence	38.7%		57.1%		0.26
Age of onset	22.2	5.6	19.3	3.4	
Cannabis					
Prevalence	25.8%		52.4%		0.08
Age of onset	18.1	4.4	19.3	6.8	
Cocaine					
Prevalence	12.9%		33.3%		0.10
Age of onset	20.5	2.9	20.1	4.9	
Stimulants					
Prevalence	6.5%		19.0%		0.21

Variable	Non-psychopaths (n=31)		Psychopaths (n=21)		p
	Mean	**S.D.**	**Mean**	**S.D.**	
Age of onset	17.0	1.4	22.0	6.3	
Opioids					
Prevalence	9.7%		33.3%		0.07
Age of onset	20.7	5.1	21.9	6.7	
Sedatives					
Prevalence	3.2%		9.5%		0.56
Age of onset	27		21.0	1.4	
Hallucinogens					
Prevalence	3.2%		23.8%		0.03
Age of onset	20		18.6	2.5	

[a]based on hand usage questionnaire (71)

[b]based on Shipley Institute of Living Scale (72),

[c]based on Welsh Anxiety Scale,

[d]based on diagnosis of abuse or dependence in the Structured Clinical Interview for DSM-IV Disorders (24). P-values for race distribution, handedness distribution, and substance abuse prevalence were computed with Fisher's Exact Test. All other p-values are based on t-tests (means presented followed by standard deviations). P-values were not calculated for substance abuse age of onset due to relatively small sample sizes of abusers for most substances.

Table 2

Clusters of significant thinning in psychopaths

Cluster number	Hemi-sphere	Location	Peak vertex Talairach (x, y, z)	Clusterwise p-value	Size (mm^2)
1	Left	Medial Superior Frontal Gyrus	−7.9, 32.3, 36.3	0.049	406.6
2	Left	Anterior Insula/Superior Temporal Gyrus	−40.9, −10.4, −11.3	0.0001	1589.5
3	Left	Fusiform Gyrus	−35.7, −18.6, −20.4	0.0065	594.1
4	Left	Lateral Occipital Cortex	−26.9, −91.8, −6.5	0.0072	585.7
5	Left	Precentral Gyrus	−47.6, −8.3, 32.7	0.0001	1566.4
6	Left	Posterior Insula/Superior Temporal Gyrus	−61.0, −18.0, 2.7	0.0058	603.5
7	Left	Dorsal Anterior Cingulate Cortex	−5.3, 32.0, 16.9	0.0015	714.2
8	Left	Lateral Superior Frontal Gyrus/Middle Frontal Gyrus	−23.9, −4.1, 40.8	0.018	498.3
9	Left	Temporal Pole	−46.3, 5.0, −27.1	0.030	453.9
10	Right	Precentral Gyrus	31.8, −16.4, 41.5	0.0004	922.2
11	Right	Temporal Pole	35.7, 14.2, −26.9	0.0023	754.3
12	Right	Posterior Superior Temporal Gyrus	55.8, −19.3, 5.8	0.008	645.1
13	Right	Inferior Frontal Gyrus	43.9, 36.1, 2.5	0.0018	797.4